

ACCELERON AEROSPACE JOURNAL (AAJ)

E-ISSN: 2583-9942 (Online) | Accessible at www.acceleron.org.in

Volume 5, Issue 4, (pp.1447-1461) Article ID: AAJ.11.2106-2555 Research Paper

https://doi.org/10.61359/11.2106-2555



Computational Outcome Validation & Evaluation of a Transport Aircraft Analysis

Asokan K *0, Jyothi NT †0, JV Muruga Lal Jeyan †0

¹ PhD Scholar, European International University – France, Paris.

² President – LIPS Research & DLCARD.

³ Research Supervisor, European International University- France, Paris.

Abstract: The results of a computational study that was carried out to examine Euler flow over a traditional transport aircraft are covered in this paper. At Mach 0.15, the analysis has been carried out for a range of angles of attack and sideslip combinations. CFD ACE+ Navier Stokes solver is used for analysis and simulation. The angle of attack has been changed in 6-degree increments from 0 to 18 degrees for sideslip values of 0, 6, and 12. The computations are performed using the Origin 3000, an SGI server. A recent study on grid independence demonstrated that a mesh size of 2,079,082 cells was optimal for achieving accurate computational results in fluid dynamics simulations. This determination was based on a systematic refinement approach, where various mesh configurations were evaluated for their impact on solution convergence and accuracy. The analysis revealed that this specific cell count effectively balanced computational efficiency with numerical precision, as further refinement yielded diminishing returns with respect to error reduction. Additionally, the use of this ideal mesh size minimized resource consumption while ensuring that key flow characteristics were captured without significant artifacts or discrepancies often associated with coarser grids. Ultimately, the findings underscore the importance of meticulous grid selection in simulation practices to enhance robustness and reliability in predictive modeling across engineering applications.

Table of Contents

1. Introduction	1
2. Methodology	2
3. Results and Discussion	3
4. Conclusion	
5. References	
6. Conflict of Interest	
7. Funding	
· · · · · · · · · · · · · · · · · · ·	

1. Introduction

The aerodynamic performance and stability characteristics of transport-category aircraft are fundamentally governed by complex three-dimensional flow phenomena that evolve with changes in angle of attack and sideslip, even at low Mach numbers typical of subsonic cruise and approach conditions. Advances in Computational Fluid Dynamics (CFD) have made high-fidelity, parametric evaluation of these regimes both tractable and repeatable, enabling engineers to quantify lift, drag, and stability derivatives with controlled numerical error while reducing reliance on costly wind-tunnel campaigns during early design phases. Within this context, Euler-based solutions. when paired with careful grid-convergence practices. remain valuable for isolating inviscid flow physics, pressure-driven loading, and global force/moment trends across configurations and flight attitudes of interest.

This study investigates Euler flow over a representative subsonic transport aircraft at Mach 0.15 across systematically varied angles of attack $\alpha \in \{0^{\circ}, 6^{\circ}, 12^{\circ}, 18^{\circ}\}$ and sideslip $\beta \in \{0^{\circ}, 6^{\circ}, 12^{\circ}\}$, using the CFD-ACE+ Navier–Stokes solver configured for inviscid analysis with stringent convergence criteria 10^{-4} on residuals. The geometry features a T-tail and fuselage-mounted engines, with GA(W)-2 and NACA 0012 airfoils assigned to the wing and empennage, respectively, reflecting canonical transport-aircraft design traits for which comparative literature and validation practices are well established. A structured grid-independence campaign determined an optimal mesh of 2,079,082 cells, balancing numerical accuracy and computational efficiency, after demonstrating diminishing returns relative to a finer 3.35-million-cell grid and measurable improvement over a 1.02-million-cell baseline.

The analysis centers on surface pressure distributions, sectional Mach contours, and derived aerodynamic coefficients C_L , C_D , C_Y and moments C_{pitch} , C_{roll} , C_{yaw} , with particular attention to stability-relevant slopes and residual asymmetries at elevated angles of attack. The results exhibit the expected linear lift trends with reduced slope versus the theoretical 2π due to finite-wing and three-dimensional effects, physically consistent drag polars across

[‡]Research Supervisor, European International University- France.

Article History: Received: 29-Sep-2025 || Revised: 16-Oct-2025 || Accepted: 16-Oct-2025 || Published Online: 30-Oct-2025.

^{*}PhD Scholar, European International University – France, Paris. Corresponding Author: |ijpsbsm@gmail.com.

[†]President – LIPS Research & DLCARD.

 β , and side-force behavior that remains near zero at $\beta=0^\circ$ while scaling linearly with sideslip as symmetry is broken. Rolling and pitching moment derivatives are negative, indicating positive lateral and longitudinal static stability in the examined envelope, whereas the yawing moment slope is positive, supporting directional stability and aligning with the lateral–directional coupling inferred from the pressure and streamline fields. Collectively, these findings substantiate the suitability of the chosen inviscid modeling approach and mesh strategy for early-phase performance and stability screening of transport configurations, while outlining clear pathways for future viscous and Reynolds-number–sensitive refinements where boundary-layer physics and separation become mission-critical.

2. Methodology

Computational Fluid Dynamics

Computational Fluid Dynamics (CFD) methodology involves a series of steps to numerically analyze fluid flow and related phenomena. It begins with defining the problem, including geometry, flow type, and boundary conditions, followed by creating a computational mesh to discretize the domain. Physical modelling specifies fluid properties and relevant physics, after which the governing equations—typically the Navier—Stokes equations representing conservation of mass, momentum, and energy—are discretized using suitable numerical methods. The solution is computed iteratively, with results analyzed and visualized through post-processing. Finally, validation and optimization ensure accuracy and reliability by comparing results with experimental or analytical data, refining models as needed for improved performance and realism.

Aircraft Description

The analysis has been carried out on a subsonic transport aircraft model. The model has 30 meters length and has 20 meter span. It has a T-Tail configuration and fuselage mounted power plants. The wing airfoil used is GA (W)-2 and tail has NACA 0012 airfoil. The geometric feature of the aircraft is summarized below.

Table-1 Geometric Parameters of the Baseline Transport Aircraft

Parameter	Value		
Overall length	30 m		
Full Span	20 m		
Root chord	4.3m		
Tip chord	1.09m		
Wing Airfoil	GA (W) 2		
Tail Airfoil	NACA0012		
Wing gross area	50 m2		
Sweep back angle	27 deg		

Grid Independence Study

Grid sensitivity analysis is conducted to identify an optimal mesh with a sufficient number of tetrahedral cells, ensuring that the solution becomes independent of grid size. Initially, a coarse mesh with an arbitrary number of cells is chosen. Subsequently, the number of cells is incrementally increased in steps. The impact of these refinements on the solution is analyzed and compared with previous meshes. This iterative process continues until the difference in results between two consecutive grids becomes negligible. In the current study, three different mesh sizes were employed: starting with a coarse grid containing 1,019,238 tetrahedrons, followed by a medium mesh with 2,079,082 cells, and finally a fine mesh consisting of 3,353,609 cells. Grid-convergence study established an optimal mesh density of 2,079,082 computational cells.

Boundary Conditions



Wall

The aircraft's surface is represented as a wall boundary with the velocity set to zero.

Outlet

The outlet boundary condition is specified as a far-field subtype, enabling the definition of static pressure, temperature, and velocity components in all three spatial directions.

Far Field

This outlet subtype is used when there is a possibility of flow entering through the boundary. It enables specifying the velocity for incoming flow at the boundary.

Convergence Criteria

Convergence criteria are selected as 10^{-4}

3. Results and Discussion

Pressure variations over the surface of the aircraft, as illustrated in Figures 1, 2, and 3, play a critical role in understanding aerodynamic performance and stability. These figures depict static pressure distributions at varying phases of flight, revealing how airflow interacts with the aircraft's geometry. A detailed analysis shows that regions of low static pressure correspond to areas of high velocity flow, particularly over wings and control surfaces during maneuvers. Conversely, higher static pressures are typically observed on the lower surfaces or installed conditions. Such pressure gradients directly influence lift generation and drag characteristics, emphasizing their importance in aircraft design and operational efficiency. Understanding these complexities allows engineers to optimize airfoil shapes and improve overall performance, thereby enhancing safety and effectiveness in various flight scenarios.



Figure 1 Surface pressure distribution at β =0, α =0

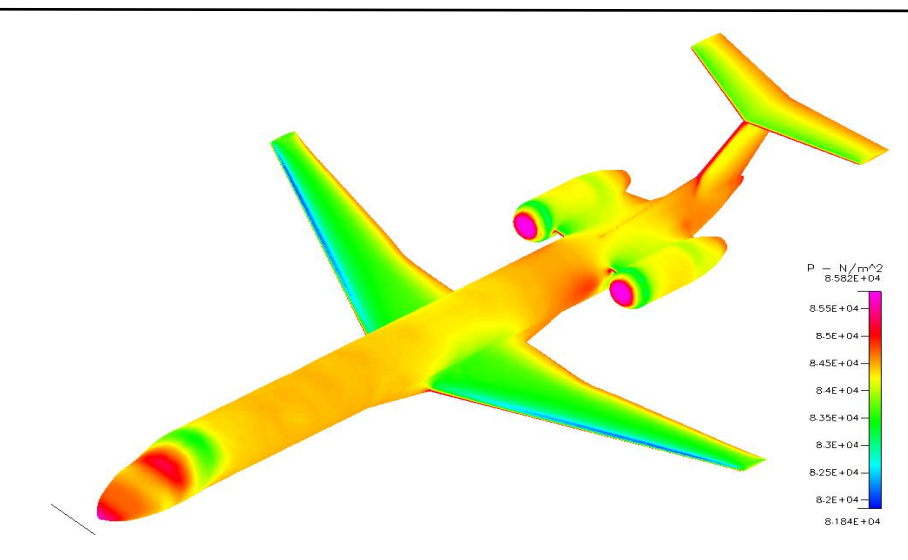


Figure 2 Surface pressure distribution at β =0, α =6

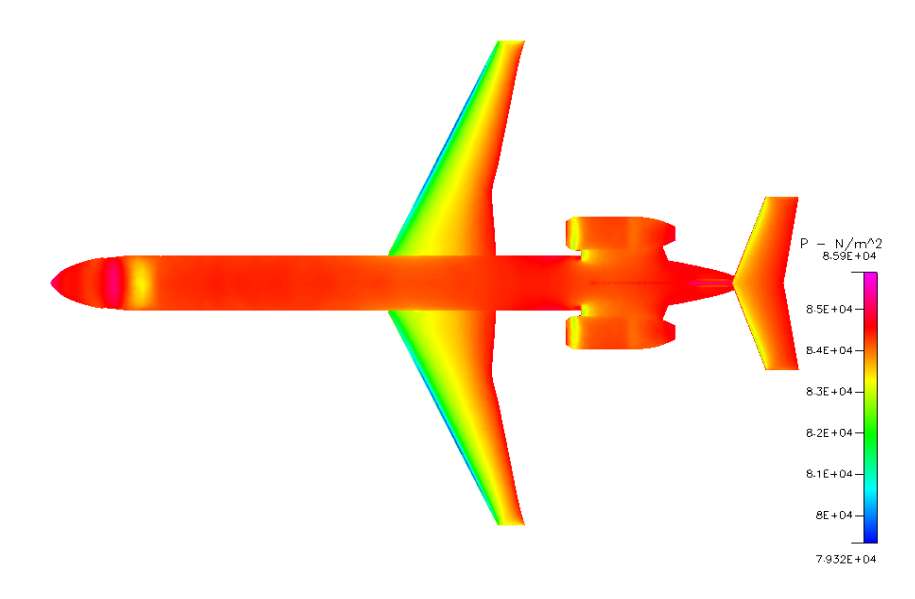


Figure 3 Surface pressure distribution at β =0, α =12

Surface pressure distributions across the aircraft are illustrated in Figures 1, 2, and 3. Static pressure increases are evident at critical stagnation regions, including the nose, windshield, and the leading edges of both the wing and tail surfaces. The figures clearly demonstrate the anticipated pressure reduction on the wing's upper surface, consistent with lift generation principles. These pressure differentials become progressively more pronounced with increasing angle of attack, as clearly depicted in the figures

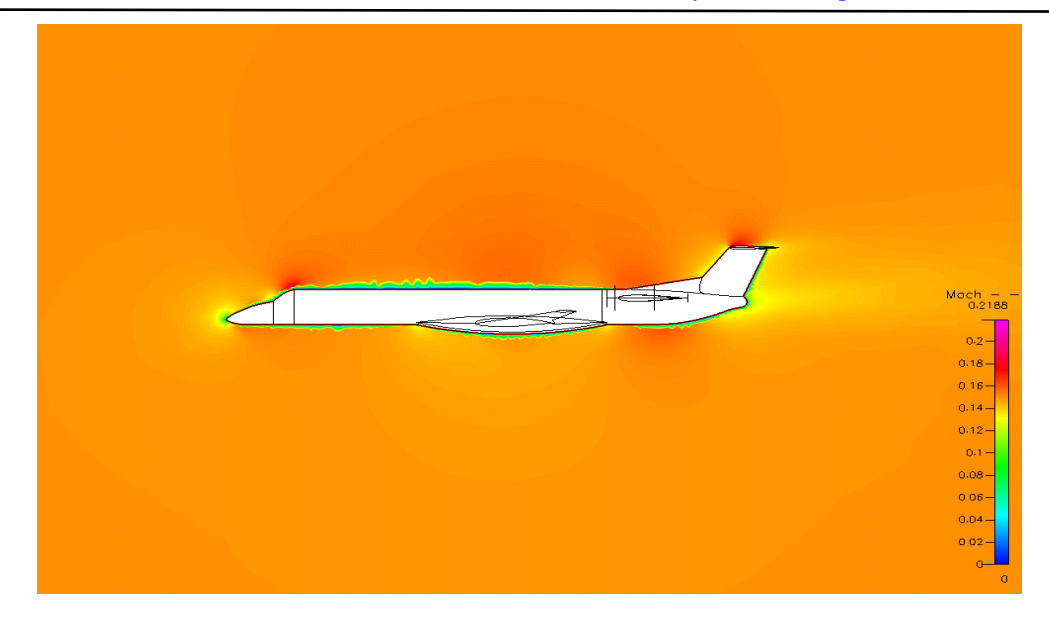


Figure 4 Mach number variation at β =6, α =6 at Y=0

Figure 4 illustrates the Mach number distribution along the section at y = 0, highlighting a noticeable increase over the wing and tail surface regions

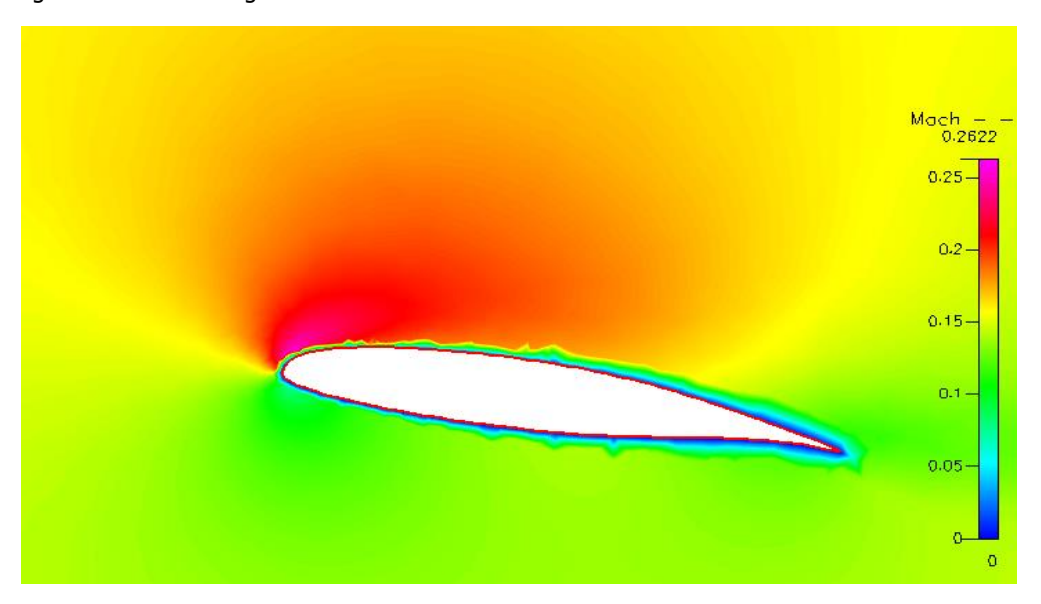


Figure 5 Mach number distribution over wing at β =0, α =12

Figure 5 shows the Mach number variation over the wing section cut at a section Y = -5.

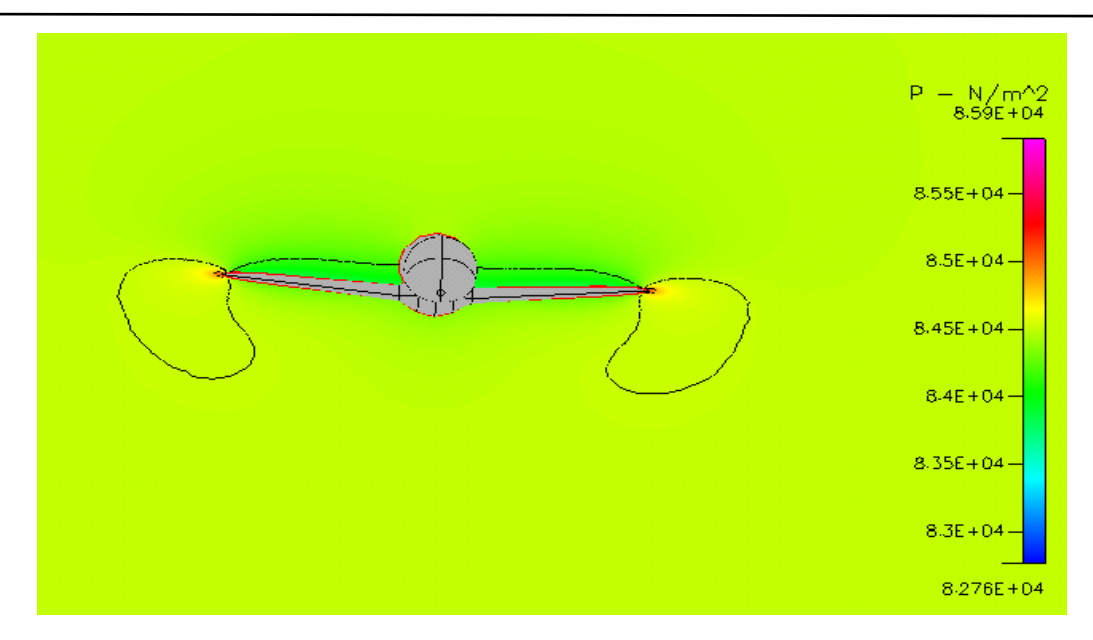


Figure 6 Pressure contours at X-cut section at β =0, α =0

Figure 6 depicts the pressure distribution under symmetric flow conditions (zero angle of attack and zero sideslip

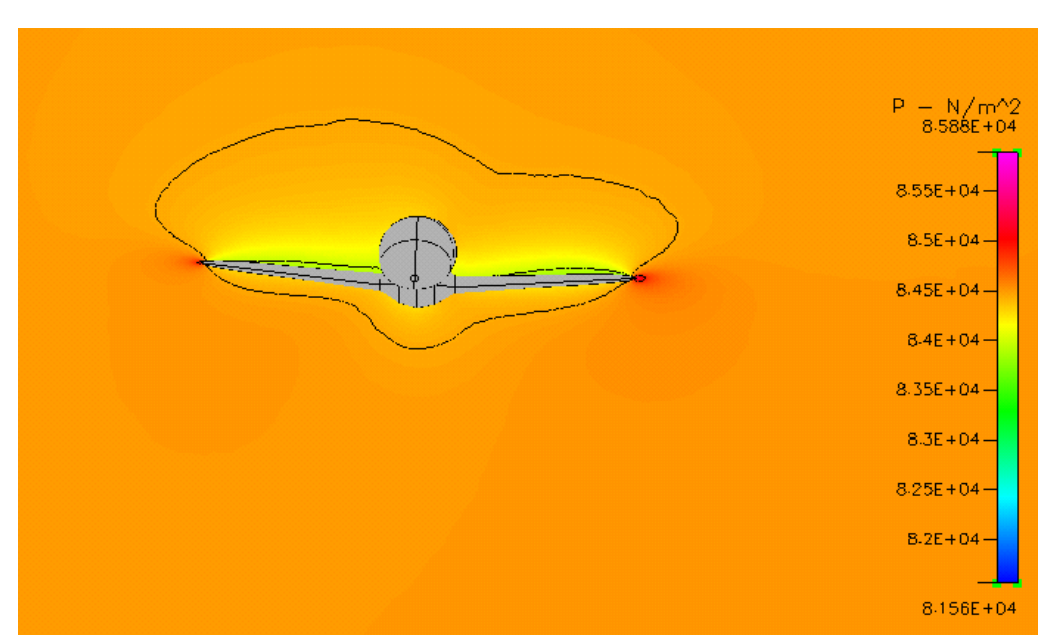


Figure 7 Pressure contours at X-cut section at β =12, α =0

Figure 7 shows the pressure contours at zero angle of attack and for a sideslip angle of 12 degrees.



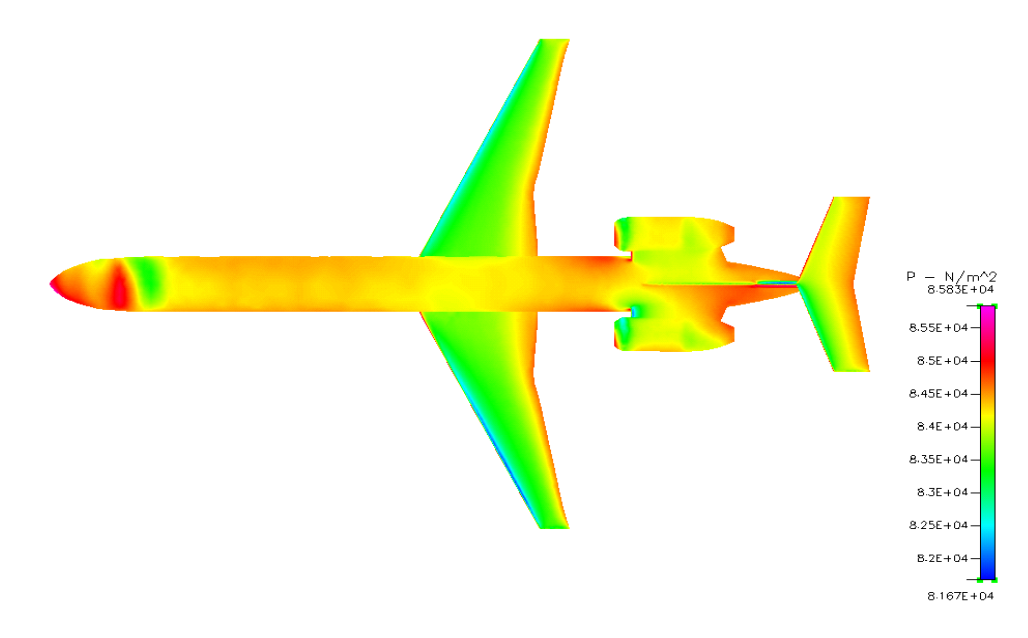


Figure 8 Surface pressure distribution at β =12, α =12

Figure 8 shows the static pressure contour at the surface of the aircraft at an Angle of attack and sideslip of each 12 degrees. The uneven pressure distribution about the longitudinal axis is clearly visible.

The above three pressure distribution plots clearly show the effect of sideslip on the flow over the aircraft.

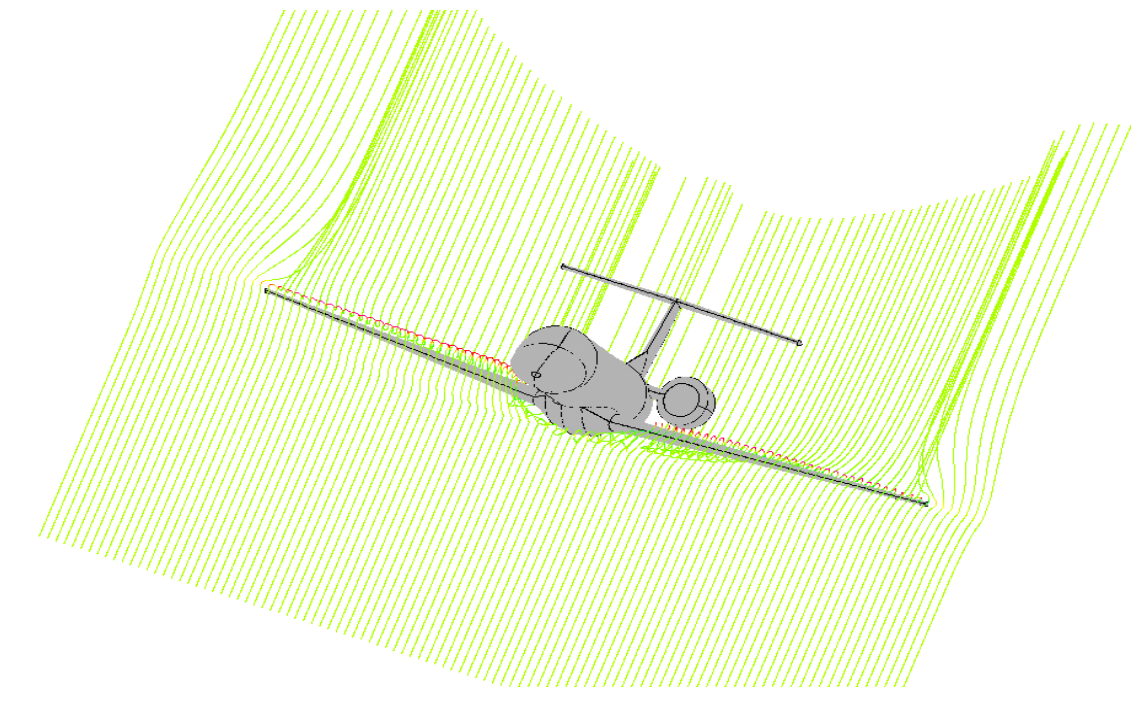


Figure 9 Flow pattern at α =6, β =6 (Mach= 0.8)

Figure 9 shows the flow pattern at an angle of attack and sideslip each 6 degrees at Mach number equal to 0.8 the streamline plot shows the wing tip vortices. The figure also shows the downwash.

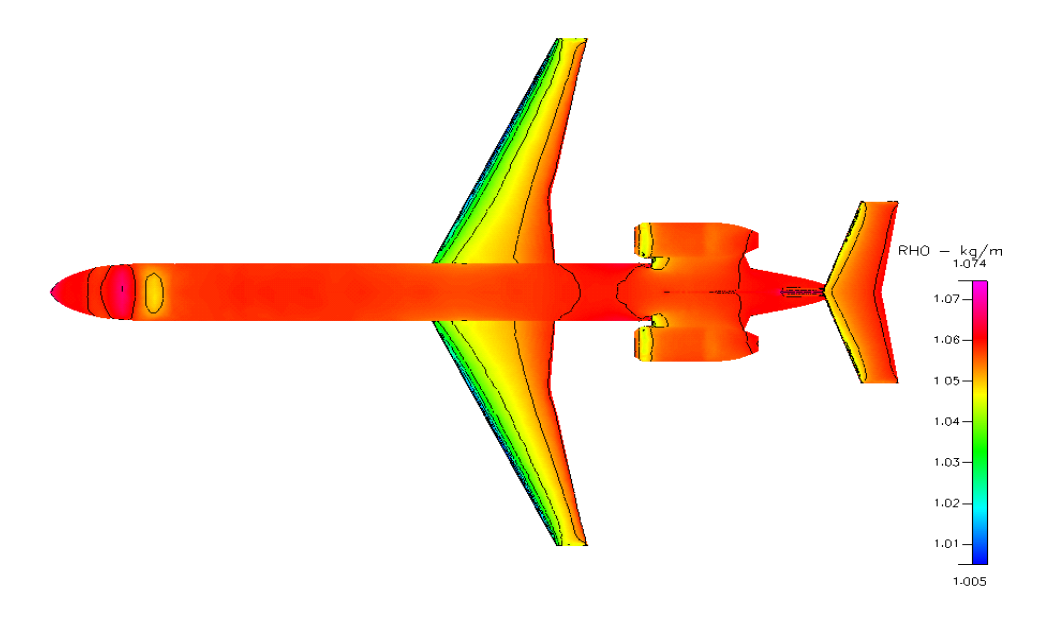


Figure 10 Density contour at β =0, α =12

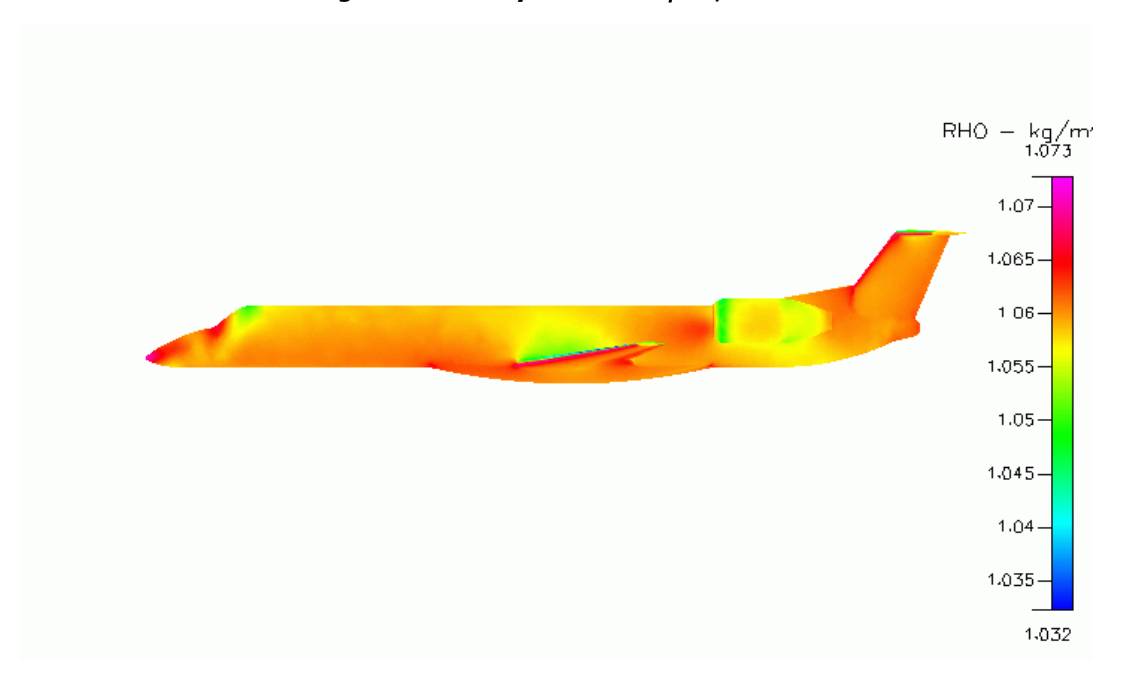


Figure 11 Density contour at β =6, α =6

Figure 10 and figure 11 shows the density contour over the surface of the aircraft at β =0, α =12 and at β =6, α =6 respectively.

The Pressure forces and Moments are estimated and calculated the non-dimensional coefficients, C_L , C_D , C_{pitch} , C_{Yaw} , C_{roll} , and C_y . These non- dimensional coefficients are plotted against angle of attack and sideslip angle.



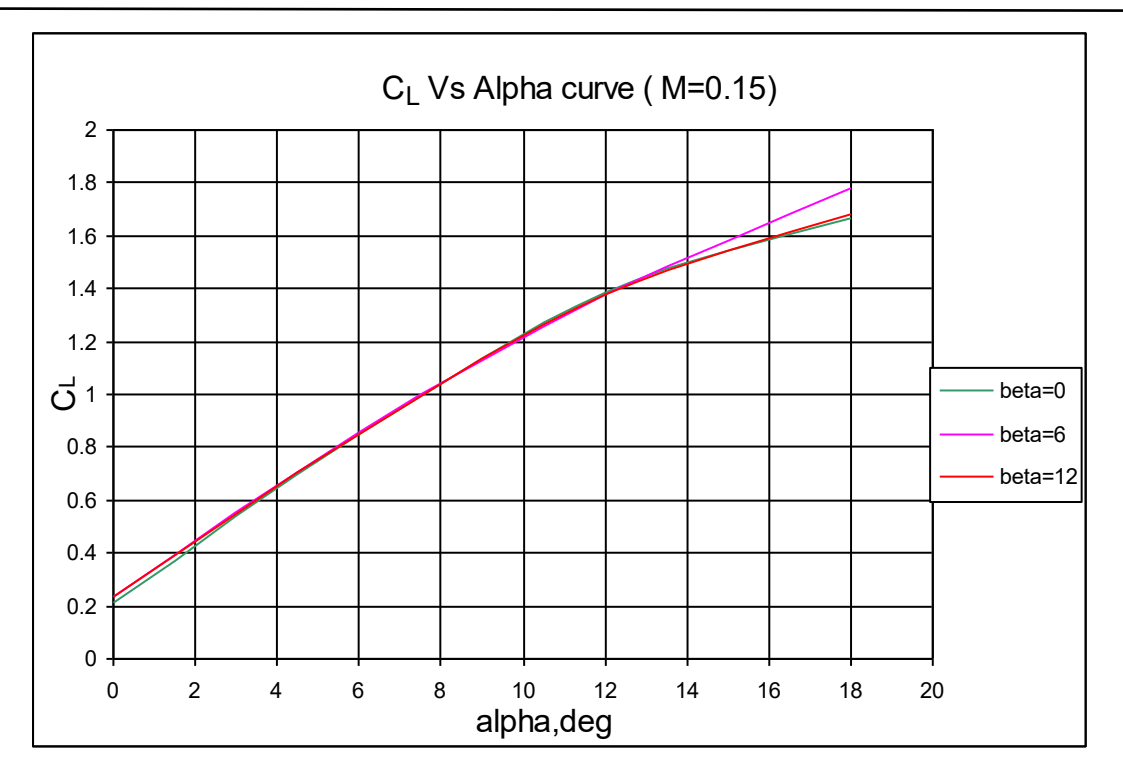


Figure 12 Lift curve

The Lift curve shown in figure 12 shows a linear variation. The lift curve is plotted for each sideslip value separately. The theoretical slope of Lift curve is 2π . The calculated slope from the result is found to be less than this value. This is justified because of the three-dimensional effect of the wing.

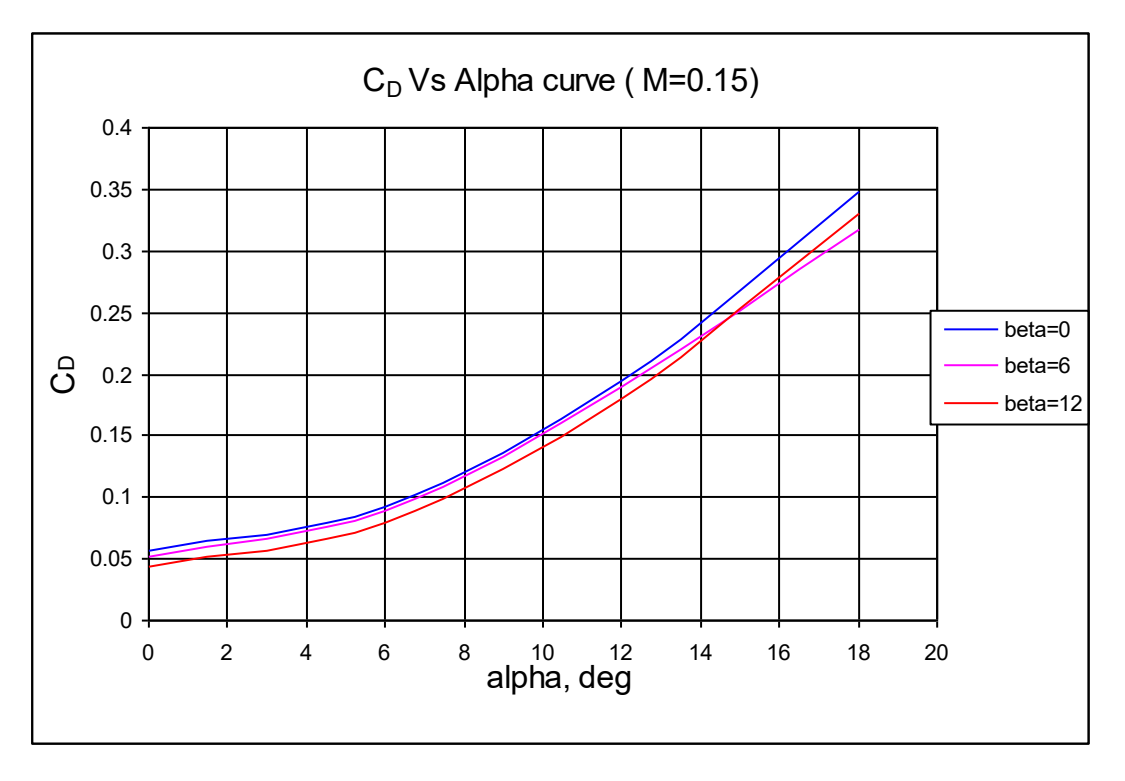


Figure 13 Drag curve

The trend of the drag curve as shown in figure 13 is as expected.

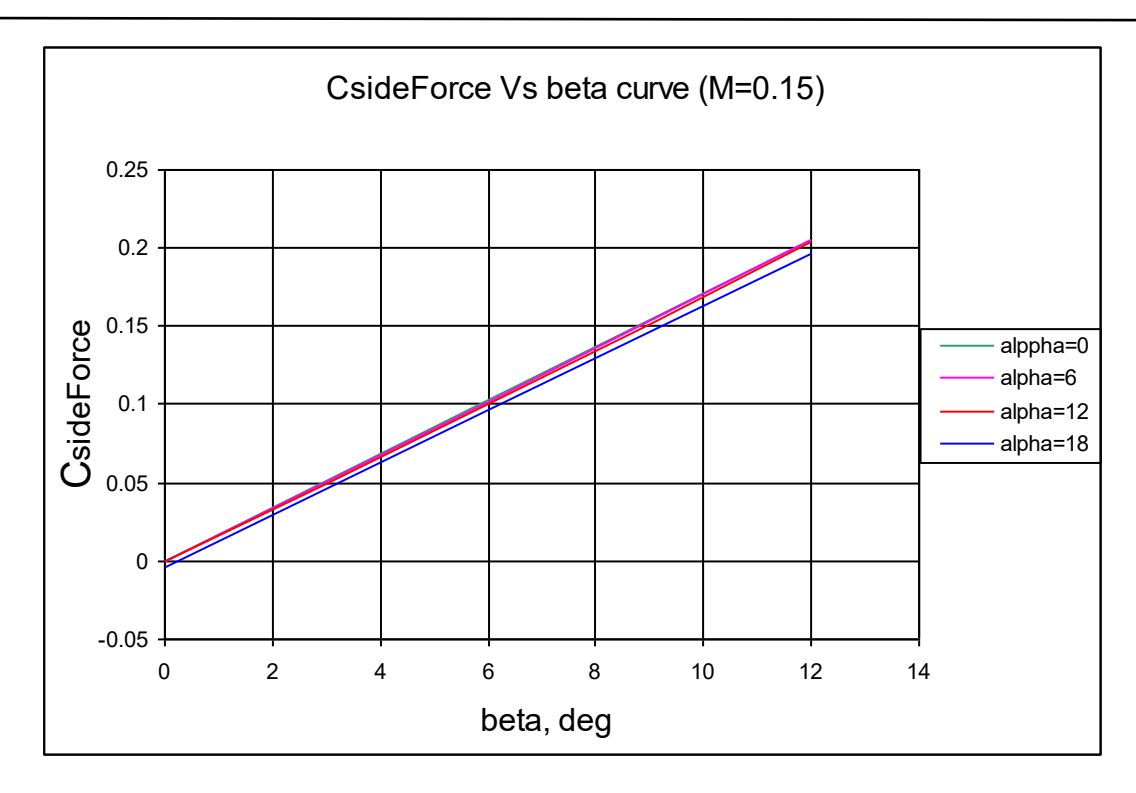


Figure 14 Side force Vs sideslip curve

The side force coefficient Vs beta curve shows a linear variation in figure 7.14. The side force coefficient is very nearly zero at zero sideslip angle.

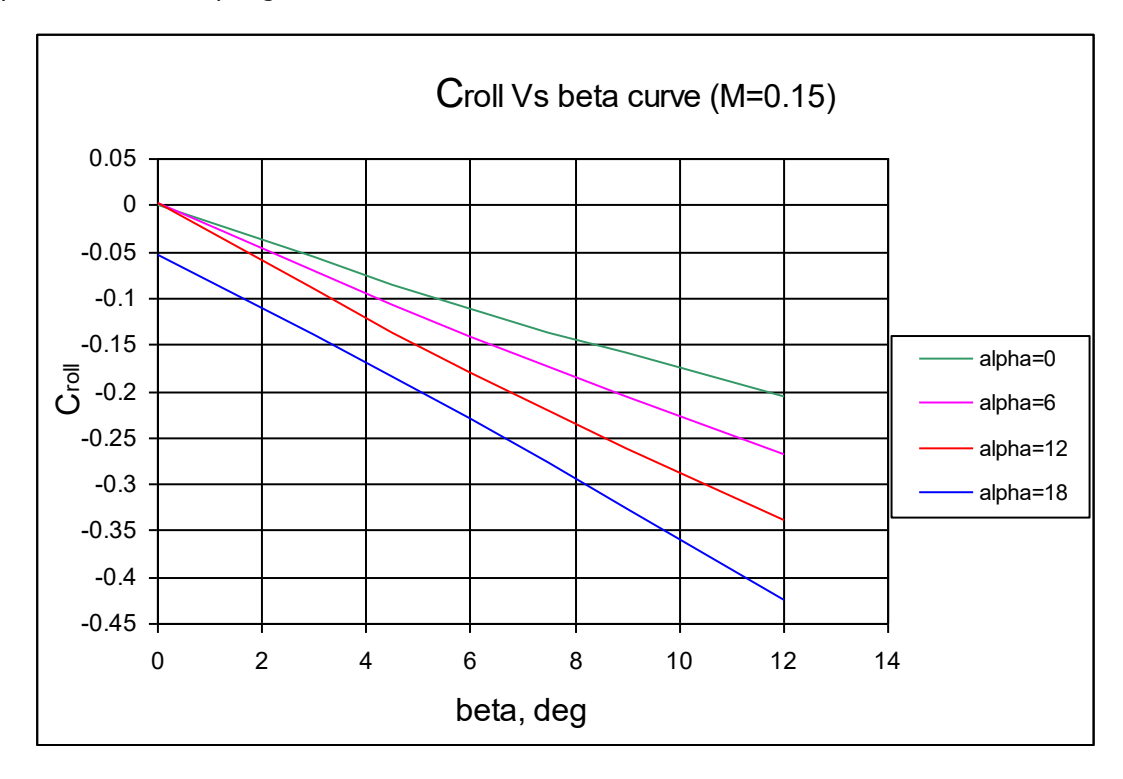


Figure 15 Rolling Moment Curve

The rolling moment curve is shown in figure 15. The negative rolling moment derivative indicates positive lateral stability, demonstrating the aircraft's inherent tendency to return to wings-level flight when subjected to sideslip disturbances. There is a modest deviation in the rolling moment at 18° angle of attack under zero sideslip

conditions. This residual rolling moment at symmetric flight conditions results from flow unsteadiness that develops at high angles of attack, although the magnitude remains relatively small.

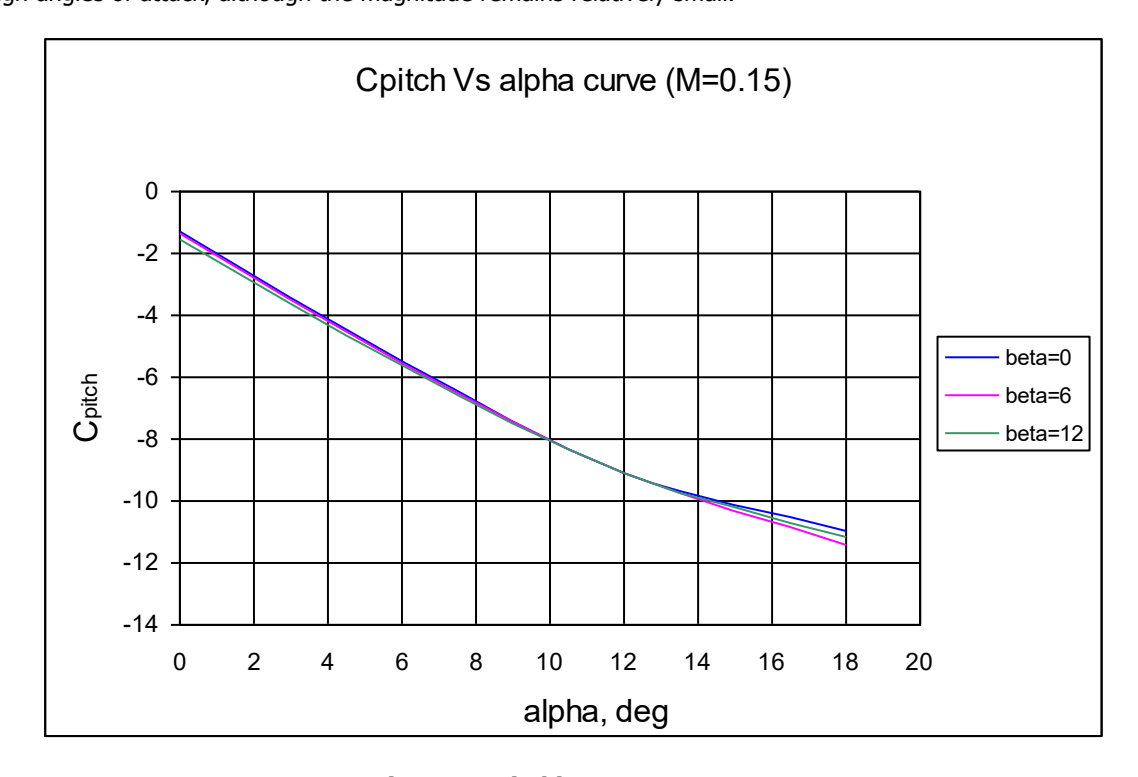


Figure 16 Pitching Moment Curve

Figure 16 presents the pitching moment curve, which exhibits a negative slope . This negative gradient indicates positive longitudinal stability, confirming the aircraft's inherent tendency to return to equilibrium following pitch disturbances confirming the aircraft's inherent tendency to return to equilibrium following pitch disturbances

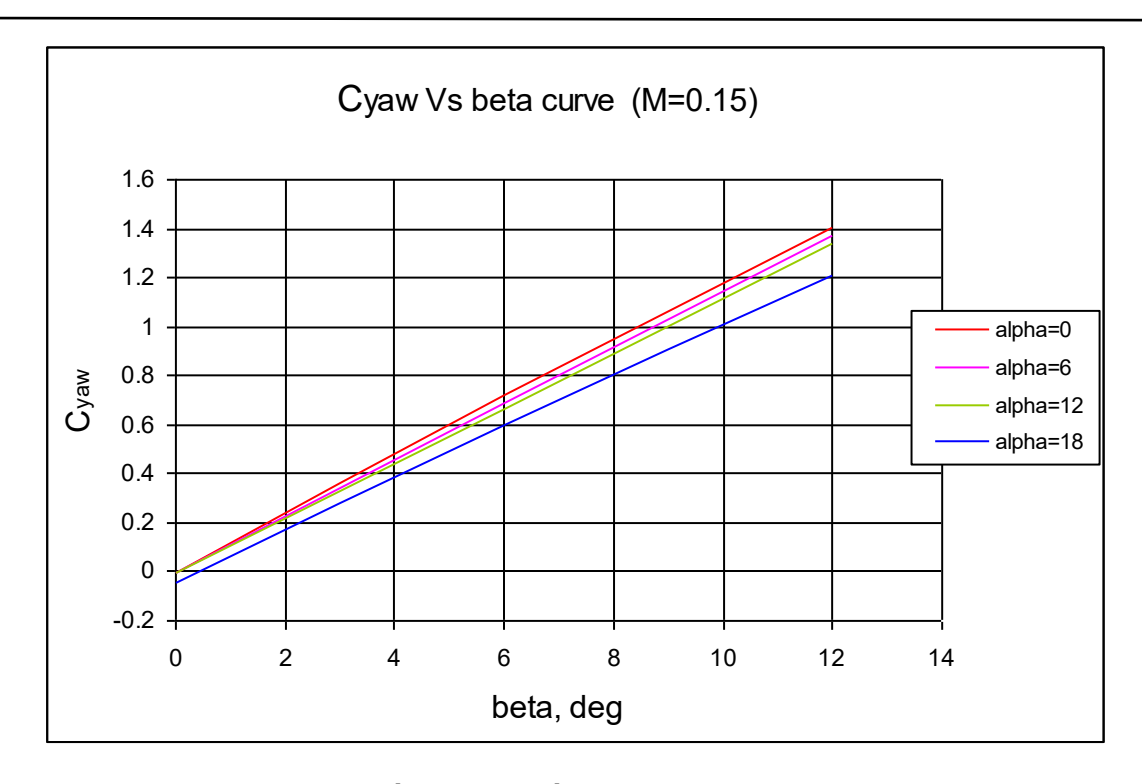


Figure 17 Yawing Moment Curve

The yawing moment curve displays a positive slope as shown in Figure 17. Notably, the data reveals residual yawing moment at zero sideslip for the 18° angle of attack condition. This phenomenon is attributed to flow unsteadiness that manifests at elevated angles of attack, as previously discussed.

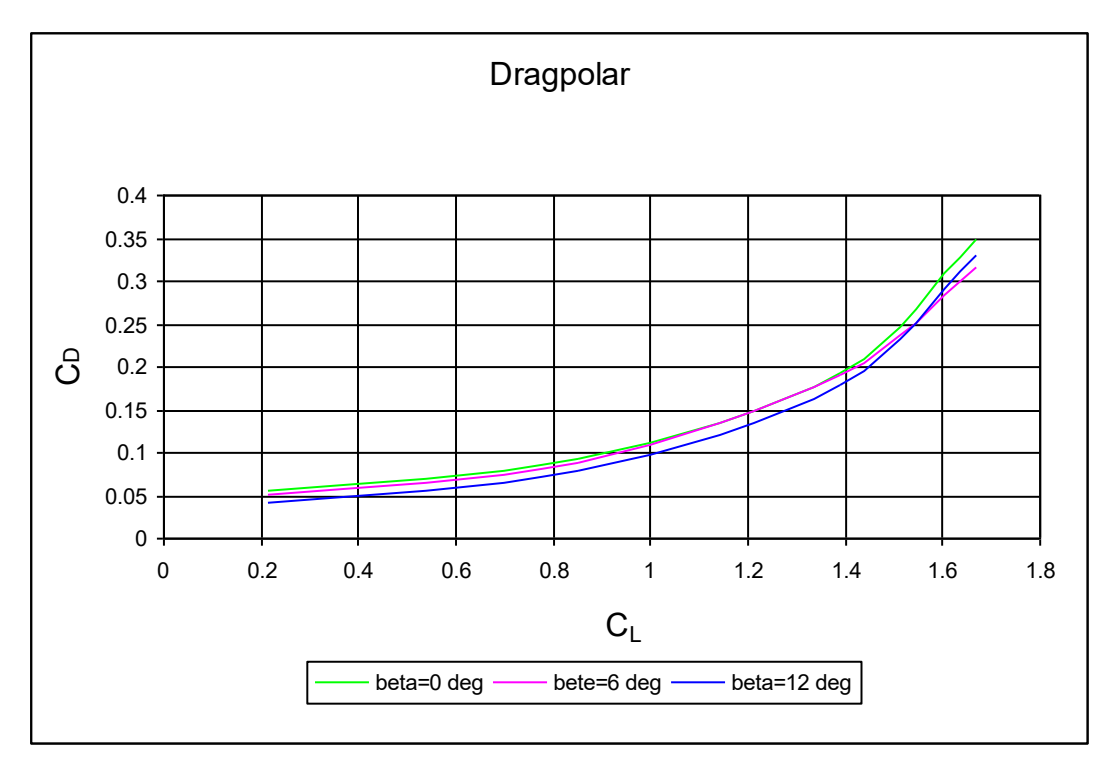


Figure 18 Drag polar

The figure 18 presents the drag polar for the aircraft across various sideslip conditions. This plot represents a fundamental design tool in aircraft development, as it characterizes the relationship between lift coefficient (CL) and drag coefficient (CD) under different flight conditions. The drag polar is essential for performance analysis, fuel efficiency optimization, and overall aerodynamic assessment of the aircraft configuration.

https://dx.doi.org/10.61359/11.2106-2555

The Table 1 shown below summarizes the aerodynamic coefficients calculated.

Beta	Alpha	CL	C _D	Cz	C _{Pitch}	C _{roll}	C _{yaw}
0	0	0.215	0.056	-0.00071	-1.2637	0.0015	-0.0023
	6	0.85	0.093	-0.0004	-5.5003	0.0027	-0.0013
	12	1.39	0.194	-0.00049	-9.0869	0.00327	-0.00128
	18	1.67	0.348	-0.0041	-10.9524	-0.0537	-0.0486
	0	0.233	0.052	0.103	-1.3421	-0.1119	0.7221
6	6	0.853	0.089	0.102	-5.5484	-0.1414	0.686
	12	1.38	0.19	0.1	-9.0869	-0.1799	0.6619
	18	1.78	0.317	0.0968	-11.4338	-0.2287	0.597
	0	0.236	0.043	0.205	-1.5225	-0.2064	1.4021
12	6	0.85	0.08	0.205	-5.6387	-0.2666	1.3721
	12	1.38	0.18	0.2046	-9.0869	-0.3388	1.3359
	18	1.679	0.33	0.196	-11.1329	-0.4249	1.2096

4. Conclusion

Euler flow over a typical transport aircraft was studied at a Mach number of 0.15 using the CFD ACE+ Navier Stokes solver. A grid independence study was completed to ensure accurate results. The angle of attack was changed from 0 to 18 degrees in steps of 6 degrees, with sideslip values of 0, 6, and 12 degrees. At zero side slip, the side force, rolling moment, and yawing moment coefficients were very small. The stability derivatives for the rolling moment and pitching moment coefficients were negative, which suggests that the aircraft has good longitudinal and lateral stability. The yawing moment curve had a positive slope, indicating that the aircraft is directionally stable. The aerodynamic coefficients were calculated, and the results show that the aircraft is stable for passengers. These coefficients and derivatives can be used for designing and calculating the aircraft's performance.

5. References

- [1] Jyothi, N. T., Nair, A., & Darney, P. E. (2023). Computational and investigational proportional flow study on Cd nozzle. International Journal for Multidisciplinary Research (IJFMR), 5(6). https://doi.org/10.36948/ijfmr.2023.v05i06.11081
- [2] Jeyan, J. V. M. L., Jyothi, N. T., & Kaushik, R. (2022). Systematic review and survey on dominant influence of Vedas and ignorance transpired in space science and aviation. International Journal of Emerging Technologies and Innovative Research (JETIR), 9(7), b490–b493. http://www.jetir.org/papers/JETIR2207158.pdf
- [3] Muthu Venkatesh, R., Rajarajan, G., Jyothi, N. T., & J. V. Muruga Lal Jeyan. (2022). Systematic survey of wind tunnel test facility in India. International Journal of Emerging Technologies and Innovative Research (JETIR), 9(6), h830–h840. http://www.jetir.org/papers/JETIR2206795.pdf
- [4] Parveen, A., Jyothi, N. T., & Jeyan, J. V. M. L. (2022). Study of implementation of value stream mapping and lean tools to achieve lean. International Journal of Creative Research Thoughts (IJCRT), 10(10), e329–e334. http://www.ijcrt.org/papers/IJCRT2210502.pdf
- [5] Jyothi, N. T., Hussainar, A., Rana, S., & J. V. Muruga Lal Jeyan. (2024). An intercontinental study of employee and employer human factor issues put up in aerospace and aviation industry. International Journal for Multidisciplinary Research (IJFMR), 6(1). https://doi.org/10.36948/ijfmr.2024.v06i01.12441
- [6] Parveen, A., J. V. Muruga Lal Jeyan, & Jyothi, N. T. (2022). International study on application of value stream mapping to identify the necessity of lean system implementation. International Journal of Scientific Research in Engineering and Management (IJSREM), 6(9).
- [7] J. V. Muruga Lal Jeyan, Jyothi, N. T., & Kaushik, R. (2022). Systematic review and survey on dominant influence of Vedas and ignorance transpired in space science and aviation. International Journal of Emerging Technologies and Innovative Research (JETIR), 9(7), b490–b493. https://www.jetir.org/papers/JETIR2207158.pdf

- [8] J. V. M. L. Jeyan, Jyothi, N. T., Raja, B., & Rajarajan, G. (2022). Theory strategy of subsonic wind tunnel for low velocity. International Journal of Emerging Technologies and Innovative Research (JETIR), 9(6), j572–j580. http://www.jetir.org/papers/JETIR2206973.pdf
- [9] J. V. M. L. Jeyan, Jyothi, N. T., Reshmitha Shree, Bhawadharanee, S., & Rajarajan, G. (2022). Theoretical study of hypersonic wind tunnel test facility in India. International Journal of Emerging Technologies and Innovative Research (JETIR), 9(6), j512–j518. http://www.jetir.org/papers/JETIR2206967.pdf
- [10] J. V. M. L. Jeyan, Jyothi, N. T., Thampuratty, V. D., Nithin, B., & Rajarajan, C. D. (2022). Concept design and development of supersonic wind tunnel. International Journal of Emerging Technologies and Innovative Research (JETIR), 9(6), j209–j217. http://www.jetir.org/papers/JETIR2206925.pdf
- [11] Muthu Venkatesh, R., Rajarajan, G., Jyothi, N. T., & J. V. Muruga Lal Jeyan. (2022). Systematic survey of wind tunnel test facility in India. International Journal of Emerging Technologies and Innovative Research (JETIR), 9(6), h830–h840. http://www.jetir.org/papers/JETIR2206795.pdf
- [12] Parveen, A., J. V. Muruga Lal Jeyan, & Jyothi, N. T. (2021). Investigation of lean developments and the study of lean techniques through event studies. International Journal for Science and Advance Research in Technology, 8(4).
- [13] Gopala Krishnan, P., J. V. Muruga Lal Jeyan, & Jyothi, N. T. (2021). Novel evaluation of aircraft data structure optimization techniques and opportunities. International Journal for Science and Advance Research in Technology, 8(4).
- [14] Upadhyay, S., J. V. Muruga Lal Jeyan, & Jyothi, N. T. (2021). Preliminary study on brain computer interface. International Journal of Innovative Research in Technology (IJIRT), 8(3), 720.
- [15] Sruthi S. Kumar, Jyothi, N. T., & J. V. Muruga Lal Jeyan. (2022). Computational turbine blade analysis with thermal barrier coating. International Journal of Engineering Research and Applications (IJERA), 12(4, Series I), 1–8. https://doi.org/10.9790/9622-1204010108
- [16] Jyothi, N. T., Ganesan, H., & Jeyan, J. V. (2024, April). Methodical assessment and truth flow analysis of wind tunnels. AIP Conference Proceedings, 3037(1), 020016. https://doi.org/10.1063/5.0196120
- [17] J. M. Lal Jeyan, Jyothi, N. T., Raja, B., & Rajarajan, G. (2022). Theory strategy of subsonic wind tunnel for low velocity. International Journal of Emerging Technologies and Innovative Research (JETIR), 9(6).
- [18] Venkatesh, M., Rajarajan, G., Jyothi, N. T., & J. V. Muruga Lal Jeyan. (2022). Systematic survey of wind tunnel test facility in India. International Journal of Emerging Technologies and Innovative Research (JETIR), 9(6).
- [19] J. M. Lal Jeyan, Jyothi, N. T., Thampuratty, V. D., Nithin, B., & Rajarajan, C. D. (2022). Development of supersonic wind tunnel. International Journal of Emerging Technologies and Innovative Research (JETIR), 9(6).
- [20] Parveen, A., J. V. Muruga Lal Jeyan, & Jyothi, N. T. (2021). Investigation of lean developments and the study of lean techniques through event studies. International Journal for Science and Advance Research in Technology, 8(4).
- [21] Gopala Krishnan, P., J. V. Muruga Lal Jeyan, & Jyothi, N. T. (2021). Novel evaluation of aircraft data structure optimization techniques and opportunities. International Journal for Science and Advance Research in Technology, 8(4).
- [22] Parveen, A., J. V. Muruga Lal Jeyan, & Jyothi, N. T. (2022). International study on application of value stream mapping to identify the necessity of lean system implementation. International Journal of Scientific Research in Engineering and Management (IJSREM), 6.
- [23] J. V. Muruga Lal Jeyan, Jyothi, N. T., & Rajarajan, G. (2022). Theoretical study of hypersonic wind tunnel test facility in India. International Journal of Emerging Technologies and Innovative Research (JETIR), 9(6).
- [24] J. V. Muruga Lal Jeyan, Jyothi, N. T., & Rajarajan, G. (2022). Theory strategy of subsonic wind tunnel for low velocity. International Journal of Emerging Technologies and Innovative Research (JETIR), 9(6).
- [25] Venkatesh, M., Rajarajan, G., Jyothi, N. T., & J. V. Muruga Lal Jeyan. (2022). Systematic survey of wind tunnel test facility in India. International Journal of Emerging Technologies and Innovative Research (JETIR), 9(6).
- [26] J. V. Muruga Lal Jeyan, Jyothi, N. T., Thampuratty, V. D., Nithin, B., & Rajarajan, C. D. (2022). Development of supersonic wind tunnel. International Journal of Emerging Technologies and Innovative Research (JETIR), 9(6).
- [27] J. V. Muruga Lal Jeyan, Jyothi, N. T., & Kaushik, R. (2022). Systematic review and survey on dominant influence of Vedas and ignorance transpired in space science and aviation. International Journal of Emerging Technologies and Innovative Research (JETIR), 9(7).
- [28] J. V. Muruga Lal Jeyan, Jyothi, N. T., Thampuratty, V. D., Nithin, B., & Rajarajan, C. D. (2022). Concept design and development of supersonic wind tunnel. International Journal of Emerging Technologies and Innovative Research (JETIR), 9(6).
- [29] Jyothi, N. T., Ganesan, H., & J. V. Muruga Lal Jeyan. (2024). Methodical assessment and truth flow analysis of wind tunnels. AIP Conference Proceedings, 3037(1), 020016. https://doi.org/10.1063/5.0196120
- [30] Mathew, B. C., Priyanka, K. S., & J. V. M. Lal Jeyan. (2020). Computational study on chamber morphing wing concept for efficient lift at various angle of attack. 2020 International Conference on Interdisciplinary Cyber Physical Systems (ICPS), 68–71. https://doi.org/10.1109/ICPS51508.2020.00020
- [31] J. V. Muruga Lal Jeyan, & Senthil Kumar, M. (2014). Performance evaluation of yaw meter with the aid of computational fluid dynamic. International Review of Mechanical Engineering (IREME).
- [32] Lal Jeyan, J. V. M., & Senthil Kumar, M. (2014). Performance evaluation for multi-hole probe with the aid of artificial neural network. Journal of Theoretical and Applied Information Technology, 65(3).
- [33] Kaur, T., Thomas, T., Jyothi, N. T., & J. V. Muruga Lal Jeyan. (2025). An intercontinental analysis of workforce dynamics in the aviation: A human factors approach. International Journal of Aviation Management (IJAM), 3(2), 1–17. https://doi.org/10.34218/IJAM 03 02 00



- [34] Asokan, K., J. V. Muruga Lal Jeyan, & Jyothi, N. T. (2025). A systematic analysis using computational and numerical methods to examine the dynamic performance of common transport aircraft. International Journal of All Research Education and Scientific Methods (IJARESM), 13(7).
- [35] Asokan, K., Jyothi, N. T., & J. V. Muruga Lal Jeyan. (2025). A review and methodology study on computational analysis needs of a transport aircraft design. International Journal of Mechanical Engineering and Technology (IJMET), 16(4), 79–92.
- [36] Chinthiya, J. V. Muruga Lal Jeyan, & Jyothi, N. T. (2025). A study on problem formulation of outside window imaginary system in aircraft. International Journal of Advanced Research in Engineering and Technology (IJARET), 16(1), 552–568. https://doi.org/10.34218/IJARET 16 01 039
- [37] Chinthiya, J. V. Muruga Lal Jeyan, & Jyothi, N. T. (2025). Aircraft cockpit flight data graphical view opportunities: An experimental approach. International Research Journal of Modernization in Engineering Technology and Science, 7(3).
- [38] Karthikeyan, A., Darney, P. E., & Husain, Y. (2025). A study on organizational development in the hospital sector through the adoption of excellent HRM practices. Journal of Management (JOM), 12(1), 1–21. https://doi.org/10.34218/JOM 12 01 001
- [39] Chinthiya, J. V. Muruga Lal Jeyan, & Jyothi, N. T. (2025). An overview on outside window imaginary system needs in aircraft. International Journal of Advanced Research in Engineering and Technology (IJARET), 16(1), 10–19. https://doi.org/10.34218/IJARET_16_01_002

6. Conflict of Interest

The author declares no competing conflict of interest.

7. Funding

No funding was issued for this research.